

# Spin Evolution of a Young Solar Type Star

Universidad Nacional de Colombia  
Sede Bogotá

Presentado por:

Juan Camilo Ibañez Mejía  
jcibanezm@unal.edu.co

Dirigida por:

Giovanni Pinzón Estrada  
Profesor Asistente  
Observatorio Astronómico Nacional  
gapinzone@unal.edu.co

Trabajo de Grado  
Facultad de Ciencias  
Departamento de Física

Julio 2010

## Resumen

Using a simplified approach to the angular momentum loss problem, we simulated the rotational evolution for a T Tauri star during the Hayashi track phase, and studied the rotational variation for different mass accretion histories. The model includes stellar contraction, mass changes, different initial conditions for the disk mass, stellar magnetic field and field geometry (i.e. the magnetically disk connected region). Three different arbitrary functions to follow the accretion rates were considered: Exponential, Hyperbolic and Power-Law, obtained via fit with the observational data of Hartmann 98 [29]. The angular speed for the weak magnetic field ( $B_* = 500G$ ) results independent for the accretion rate considered, suggesting periods around 1 – 5 days at the end of the Hayashi track ( $\sim 3Myr$ ). For the strong magnetic field case ( $B_* = 2000G$ ), with exponential and power-law accretion the resulting periods gather around 7 – 20 days, although for the hyperbolic case, the resulting periods are bigger (between 20 – 40 days). These results correlate with the general observational data. Eventhough we know that the general picture we are using its just an approximation for the original problem, one of the most relevant topics not considered is the open field topology, which leads to magnetic reconnection which gradually decreases the spin down magnetic torque felt by the star, therefore we will have again fast rotators, leaving us with the idea that there has to be another angular momentum loose process felt by the stars, like for example stellar winds.

# Índice

<b>1. Introduction</b>	<b>4</b>
<b>2. Stellar Spin Evolution Model</b>	<b>5</b>
2.1. Mass Accretion Rate . . . . .	6
2.2. Contracting Protostar . . . . .	8
2.3. Star-Disk Magnetic Coupling . . . . .	9
2.4. Torques Between Star and Disk . . . . .	9
2.5. Truncation Radius . . . . .	10
2.5.1. Truncation Radius Calculation . . . . .	10
2.5.2. System States . . . . .	11
2.6. Total Torque . . . . .	11
2.7. Numerical Simulation . . . . .	12
<b>3. Results</b>	<b>12</b>
3.1. Exponential Accretion . . . . .	13
3.2. Hyperbolic Accretion . . . . .	15
3.3. Power-Law Accretion . . . . .	17
<b>4. Conclusions</b>	<b>19</b>

# 1. Introduction

Stars have been one of the oldest and most important subject of study for mankind. During the day we see the sun as the brightest thing in the sky moving around, and in the night we see this impressive bright dotted background full of shapes. There is always someone that tries to explain what is all of that. The first idea about the Sun, and also the stars, as evolving bodies that form from a diffuse gas, was first dreamt in the 18<sup>th</sup> century when Pierre-Simon Laplace (1798) pointed that the Sun and planets where formed from a flattened and rotating gaseous nebula under the action of gravity. The Laplace idea based on the gravity shaping the primitive solar nebula, that was the first guess, but the details that comes further showed a more complexe scenario.

This idea remained unstudied until mid-20<sup>th</sup> century, which rapidly moved to a fully based subfield. In 1940 Alfred Joy, initially attracted by the low-ionization emission line spectra in the proximity of dark cloud complexes [1], identified the class of "T Tauri Variable Stars" which now are largely known as Classical T Tauri Stars (hereafter CTTS).

In the 1950s astronomers measured in most of the CTTS more energy than they expected, so an extra and a different source of energy than those radiated by the star was claimed, it remained uncertain until late 1970s, when the opening of infrared and UV windows lead observers like Merle F. Walker (1972) [2] to postulate a circumstellar disk explanation for the spectroscopic properties of these young stellar objects (YSO), he pointed out "We might expect the infall to occur in a preferential plane during the last stages of collapse of the protostellar cloud is suggested by analogy with the solar system, where the coplanar orbits of the planets indicate that the presolar nebula must have collapsed to a plane during the formation of the system".

With this new assumption, Lynden-Bell & Pringle (1974) [3] built an extremely well theoretical foundation, based on the disk picture suggested by Walker, leading to a powerfull physical and mathematical description for the circumstellar disks. But it was until late 1980s with indirect evidence of disks when this model was completely accepted and the paradigm shifted to the actual picture. The IRAS observations of CTTS confirmed the presense of dust surrounding the protostar (Beichman et al. 1986, Myers et al. 1987) and then Bertout (1987) [4] compared the observed spectral energy distribution of T Tauri Stars (hereafter TTS) with models of stars interacting with accretion disks and finally Königl (1991) [5] adapted the Ghosh & Lamb (1979) [6] magnetospheric accretion model to a TTS environment.

The conditions in which T Tauri stars are studied underline a series of constrains, as the typical masses which indicates that these stars are very similar to a young Sun before it entered into the Main Secuence. Therefore the study of TTS phase is done while they still in the Hashashi track, which is a few times 10<sup>6</sup> yr, where some constraints can be consideren to facilitate the vision.

The evolution of CTTS occurs as long as accreting matterial is falling onto the star and the star is contracting, but this single idea implies that the star is always gaining speed and this leads us to think that young stars rotate too fast, very close to the break up speed <sup>1</sup>. This fact takes us to one of the most significant problems in the study of CTTS, because obsevationes have shown that these TTS are in fact rotating an order of magnitude slower than the break up speed [7] [8], not as fast as we expected. This problem was first noted by Vogel & Kuhl (1981) [9], who measured very low velocities in a large fraction of nearly solar mass stars, for this reason they assumed that there has to be some mechanism capable of removing significant amounts of angular momentum from the star. Observations helped astronomers to explore different processes that help to understand this problem, like the idea that stars with disks rotates slower than those without disk, or the presence of eruptions that removes angular momentum from the star, but this problem is still an open question. The state of the art for this problem postulate two main ideas to explain the low rotators:

- There is an angular momentum transfer between the star and disk due to a magnetic connection between the two. The net magnetic toque is strong enough to enforce the rotation of the star towards equilibrium state. [6] [10] [5] [11] [12] [13] [14]

---

<sup>1</sup>The Break up Speed is the Keplerian Velocity at the Star's Equator  $\Omega_{BreakUp} = \sqrt{\frac{GM_*}{R^3}}$  which is the maxium speed a star can have to maintain its structure.

- There are stellar winds which remove big amounts of angular momentum from the star. [15] [16] [17] [18] [19] [20]

Even so observations have shown that both processes coexist and extract angular momentum from the star, in this work we will only focus our attention in the analysis of how the spin down magnetic torque proceeds. This magnetic coupling has been studied and developed by several authors using different approaches, like Königl (1991) [5], Cameron & Campbell 1993 (hereafter CC93), [12], Insu Yi (1995) [21] and Matt & Pudritz (2004) [22].

The magnetic braking inspider in the study of white dwarfs and neutron stars, the model was taken from the Ghosh & Lamb model [6] which calculated the torque felt by the star done via the star-disk interaction. The torque is exerted on the star due to the twisting of the field lines which are coupled to the disk. Our model of magnetic braking require more detailed treatment, because while the star is contracting as it accretes mass. Although CC93 [12], Yi [21], Armitage & Clarke (1996)[13], Matt & Pudritz [22] adapted the Ghosh & Lamb torque model to compute the spin evolution of a TTS, including contraction, decrease of accretion rate with time, changes in the magnetic field strenght and closed field topology. When the torques raised by these conditions are strong enough to enforce an equilibrium spin rate, the idea is commonly known as "Disk Locking".

Concerning the magnetic field of the star, it appears te be uncertain. First the assumption of a dipole field, neglects more complexes configurations, and it is not possible to assure the existence of a Dynamo field or a Fossil field. For example CC93 using a dynamo field configuration, found that the resulting magnetic field strenght at the end of the pre-main secuencia would be of the order of  $\sim 10^3\text{G}$ , Yi [21] worked with a more general idea in which the field could be dynamo generated, fossil field or a field regulated by the contraction of the star. The results found by Yi of magnetic field strenght where similar to those found by CC93.

Everything seemed to be fine and the "disk locking" model explained the slow rotation of accreting TTS, but everyone recognized that there was a serious theoretical problem with the Ghosh & Lamb model, which was that magnetic field lines connected to almost all the disk and become highly twisted in the azimuthal direction, then several authors showed that this twisting gives rise to the oppening of the field lines [23][24][25], which disconect the star from the disk and therefore reduces the spin-down torque on the star[26]. But the amount of the field lines oppening depends on the strenght of the coupling between the disk and the field, which is parametrized by two adjustable variables, where a good coupling generates lots of field oppening and thus reduces the spin-down torque, but a bad coupling reduces the field oppenings but is not strong enough to spin-down the star to a slow rotator as expected from observations.

For this case we are using an arbitrary function to specify the specific accretion rate, which means that this accretion is only dependent on time, this is done because the specific accretion rate, depends on the conditions of the stellar parameters at each timestep, so the right thing to do would be solving the disk equations in the same timestep than we are solving the stellar evolution equations. For our case the accretion rate is given by a function that is adjusted to accrete the disk mass in 3 Myr. We are going to use 3 different functional forms for the accretion rate and with each accretion function vary the initial conditions like initial angular velocity, taking fast rotators and slow rotators, and changing the disk mass, using high accretion rate and low accretion rate, studying the evolution for 3 Myr, and plotting the stellar parameters during this evolution.

In section 2 is a brief description of the model of stellar spin evolution, section 3 contains the general idea of the numerical simulations method used analyze the protostar, in section 4 we will present the results of the simulation and an analysis of this results and section 5 will contain the conclusions.

## 2. Stellar Spin Evolution Model

One-dimensional spin evolution models (in radius,  $R_*$ ) in the literature, consider that the angular velocity of the star  $\Omega_*$  evolves on time governed mainly by some independent mechanisms. On one side, the gravitational contraction of the protostar, bringing gradually the stellar radius from  $8R_\odot$  up to  $2R_\odot$  during the first three Myrs (as shown in fig 2 and for instance CC93 [12], MP05 [22], Matt et al 2010). Spin evolution models compute the net magnetic torque integrated onto the whole stellar surface and thus  $\Omega_*$  using the equation:

$$\frac{d}{dt}(I_*\Omega_*) = I_*\frac{d\Omega_*}{dt} + \Omega_*\frac{dI_*}{dt} = T_* \quad (1)$$

where  $I_*$  is the moment of inertia of the star. Due to the gravitational contraction this quantity is obviously dependent on time. Evolutionary models such as Siess et al. (2000) make accurate predictions for  $I_*$  and when it is used in equation (1) together with an expression for the total torque  $T_*$ , a clear picture of the evolution of the stellar rotation emerges. By assuming a constant value for  $T_*$  Bouvier et al. [7] computed solutions of (1) along the whole pre-main sequence for a set of initial stellar periods ranging from 1-10 Days. However the assumption of a constant torque independent on time seems unrealistic. This work will use the approximation presented by Cameron & Campbell in 1993, [12], in which it is assumed that the star can be described as a fully convective rotating and contracting polytrope with index  $n = 3/2$  magnetically coupled to a thin accretion disk. A detailed description for the contracting protostar is presented in section 2.2 and star-disk magnetic coupling in section 2.3.

If the moment of inertia of the star is given by  $I_* = k^2 M_* R_*^2$ , where  $k^2 \sim 0,2$  [28] is the normalized radius of gyration of the star, is easy to show that equation (1) leads to:

$$\frac{d\Omega_*}{dt} = \frac{T_*}{I_*} - \Omega_* \left( \frac{\dot{M}_a}{M_*} + \frac{2}{R_*} \frac{dR_*}{dt} \right) \quad (2)$$

where  $R_*$  is the stellar radius and  $\dot{M}_a$  is the stellar accretion rate, defined as the rate at which the star gain mass from the disk. The disk gas matter is deposited onto the stellar surface during the accretion process. The evolution of the accretion rate is an important factor for the knowledge of the stellar rotational evolution. Accretion rates have been measured on T Tauri stars with ages between 0.3-6 Myr, and have been found to follow theoretical predictions by Hartmann et al. (1998) [15], quite nicely (Sicilia-Aguilar 2006-2009). However, there is only sparse data existing covering the interestin region  $> 6Myr$  and literally there is no data for objects older than  $10Myr$ . In figure (1) we present typical values for accretion rates during the first 3 Myr and a set of three possible behaviors for the accretion process during these early stages of stellar evolution, all of them are roughly in agreement with the bulk of observational data.

## 2.1. Mass Accretion Rate

Computing  $\dot{M}_a(t)$  is not an easy task, due to the uncertainty of the accretion rate at each time. It is also difficult to determine the evolution of the mass accretion rate from observations because we cannot follow a T tauri star for its 3 Myr evolution, instead we observe a group of stars in different stages, measure the accretion rate, as shown in figure 1, and try to correlate this observations with a mass accretion evolution function, our first guess is that accretion is determined by the initial mass-content of the surrounding disk at  $t = 0$ , labeled as  $M_D$ , and determined by:

$$M_D = \int \dot{M}_a(t) dt \quad (3)$$

Where  $\dot{M}_a(t)$  is described as

$$\dot{M}_a(t) = \dot{M}_a(t_0) f(t) \quad (4)$$

where  $t_0 = 3 \times 10^5$  yr is the birth-line,  $t_f = 3$  Myr and  $\dot{M}_a(0)$  is the initial accretion rate determined by

$$M_D = \int_{t_0}^{t_f} \dot{M}_a(0) f(t) dt. \quad (5)$$

## Mass Accretion

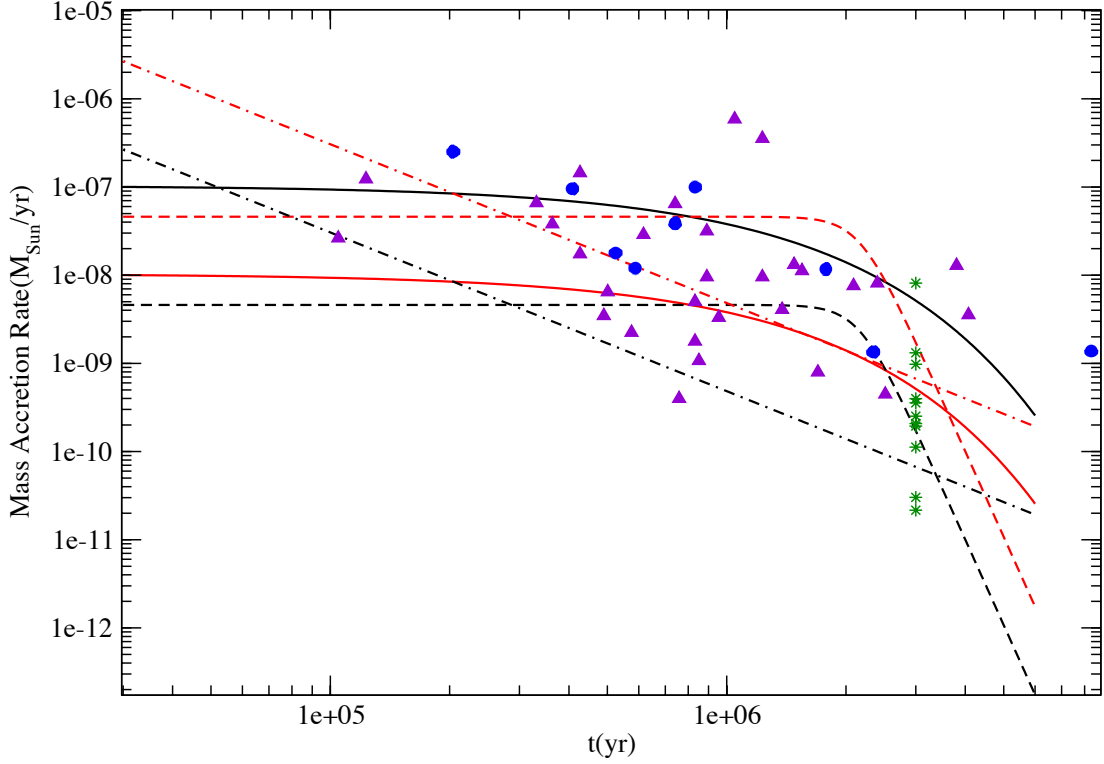


Figure 1: Accretion rates for the three different models for 6 Myr, exponential (6)(Solid Lines) , power-law (7)(dotted-dashed lines) and hyperbolic (8)(dashed lines) and two different disk masses,  $M_D = 0,1$  and  $M_D = 0,01$ , hereafter red lines represent high accretion rate, and black lines low accretion rate. This figure also includes observational data, taken from Hartmann et al 98 [29], the blue 'star (\*)' represent the data taken by blue spectrum analysis and the violet 'stars' represent data taken by photometry.

Here we will use three different functions for  $f(t)$  where the accretion rate decreases gradually from the initial value  $\dot{M}_a(t=0)$  in a timescale  $t_a$  assumed to be 1 Myr.

Assuming  $f(t)$  as

$$f(t) = e^{(-t/t_G)} \quad (6)$$

$$f(t) = \left(\frac{t}{t_0}\right)^{-\eta} \quad (7)$$

$$f(t) = \frac{1 + \tanh[5 - \log(\frac{t}{t_G * 0,04})]}{2} \quad (8)$$

where  $\tau = t/t_G$  is a dimensionless time parameter. The initial accretion rate  $\dot{M}_a(0)$  is different for each case, for the exponential and power-law cases, we find  $\dot{M}_a(0)$  solving equation (5), but for the Hyperbolic case are difficult so we adjusted the initial value numerically. Observations [29] predicts analytic solutions accretion rates approximately  $\sim 10^{-7} M_\odot/\text{yr}$  but as already seen before this is for different initial conditions and stages of

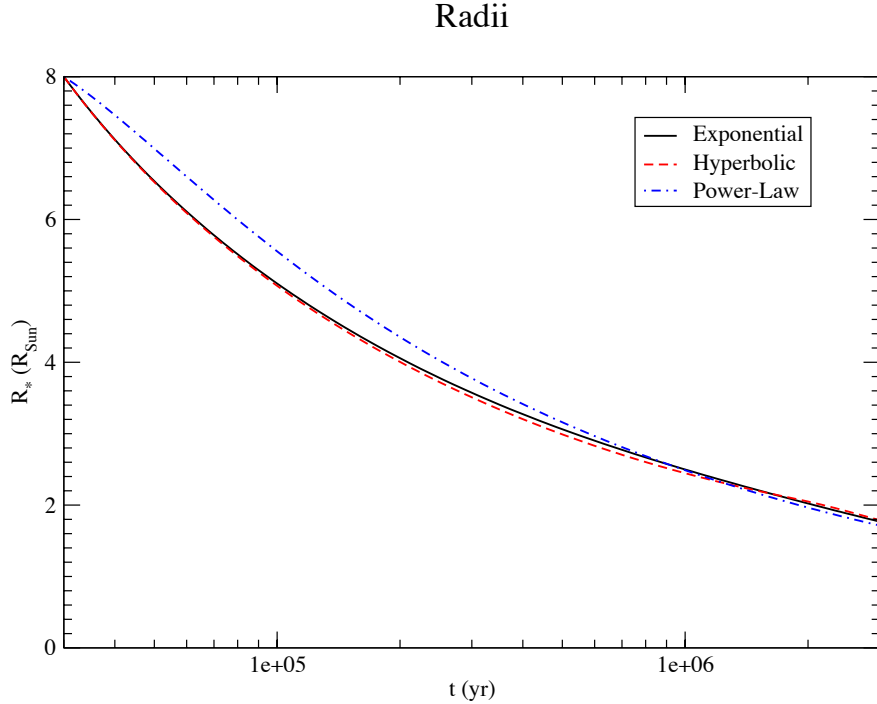


Figure 2: Radii Variation with Time for the three accretion Models normalized to solar units, Solution for the equatin (9) are represented by solid Lines for Exponential Accretion, dashed line for Hyperbolic Accretion and dotted-dashed line for Power-Law Accretion.

the evolution. This three models showed in figure 1 for accretion rate represent an exponential decrease, rapid decreasing powerlaw and a nearly constant hyperbolic accretion rate with a sudden decrease.

Figure (1) represents the evolution of the accretion rate at  $3 \times 10^6$  Myr for the three different models already discussed. For each model we considered two different disk masses  $M_D = 0,1M_\odot$  and  $M_D = 0,01M_\odot$ , in order to compare two extreme accretion rates. In figure (1) high accretion represented by red lines, and low accretion represented by black lines. The mass was always considered to a final mass of  $M(t_f) = M_\odot$

## 2.2. Contracting Protostar

Cameron & Campbell [12] did a detailed study of the stellar rotation of a CTTS along the 'Hayashi-Track', the evolutionary path traced by a PMS of a fixed mass during their early evolution on the HR diagram. For low mass stars this track has been observed to be approximately a vertical line in such diagram i.e. the protostar evolves during 'Hayashi-Track' at constant effective temperature. The CC93 [12] model assumes that half of the black body and half of the energy thermalizes the surface of the star. Under such circumstances, a relation between contraction and 'Radiation' can be easily obtained

$$\frac{dR_*}{dt} = \frac{2R_*\dot{M}_a}{M_*} - \frac{28\pi\sigma R_*^4 T_e^4}{3GM_*^2} \quad (9)$$

where  $G$  is the Newton's gravitational constant and  $\sigma$  is the Stefan-Boltzmann constant,  $\dot{M}_a$  is the mass accretion rate and  $T_e$  is the effective temperature. Figure (2) shows the radii evolution for the three different models, with an initial radii of  $R = 8R_\odot$  and effective temperature  $T_e = 4280K$  [27].



### 2.3. Star-Disk Magnetic Coupling

We now that the star-disk system is composed for a star (described as a rotating solid body), and a thin keplerian disk around the star, in which the angular momentum vector of the star and disk are aligned. As we now the star rotates as a fraction of its break-up speed <sup>2</sup>, but as the disk is keplerian, rotates at a different speed from the star at all radii, except at the corotation radius given by

$$R_{co} = f^{-2/3}R_*, \quad (10)$$

where  $r$  measured radially outward from the center of the star, we know that for  $r < R_{co}$  the disk rotates faster than the star, and for  $r > R_{co}$  the disk rotates slower than the star.

A rotational axis aligned dipole magnetic field is assumed for the model, it is attached to the stellar surface and it also connects to the disk. In this configuration the magnetic field connects the star to the disk everywhere. The magnetic lines will therefore be azimuthally twisted, except for  $R_{co}$ , giving rise to torques between the two. For  $r < R_{co}$  the connected region in the disk will exceed the star, this will generate a field line twisting which arise spin up torques felt by the star (and spin down the disk). For  $r > R_{co}$  the field lines will produce a spin down torque to the star (and spin up the disk). The term "coupling" could be used to indicate that there are field lines frozen to the disk. Matt & Pudritz [18] showed that the strength of this coupling could lead to the opening of field lines due to the varying topology of the magnetic field. They measured the twist of  $B_*$  and used the parameters  $\beta$  and  $\gamma_c$  to describe it. The parameter  $\gamma \equiv B_\phi/B_z$  where  $B_\phi$  is the azimuthal component of the magnetic field.  $B_z$  is the magnetic field strength in the equatorial plane given by

$$B_z = B_* \left( \frac{R_*}{R} \right)^3. \quad (11)$$

$\gamma$  quantifies the twist of the field lines at the surface of the disk, the maximum possible value is  $\gamma_c = 1$  [14] gives rise to the opening of field lines when  $B_\phi = B_z$ . But for this work we will only consider a closed topology in which  $\gamma = \gamma_c = \infty$ , but the growth of the  $B_\phi$  component depends on the strength of the coupling between the field lines and the disk, because magnetic forces act to resist the twisting so there can be azimuthal slipping of the field lines through the disk, which is represented by the dimensionless parameter  $\beta$  given by

$$\beta = \frac{\eta_t}{h v_k} \quad (12)$$

where  $\eta_t$  is the magnetic diffusivity,  $h$  is the disk thickness and  $v_k$  is the keplerian rotation velocity. Large values of  $\beta$  correspond to weak magnetic coupling, and small values, to a strong coupling.  $\beta$  is a highly unknown parameter, but Matt & Pudritz [18] suggested that  $\beta = 0,01$  would be a reasonable value for pre main sequence stars. Here I am going to take  $\beta = 1$  because most of the models adopt parameters that give similar results to [18] with  $\beta = 1$  [13].

### 2.4. Torques Between Star and Disk

The interaction between the star and disk generates a series of torques, as it was mentioned before, analyzing the torques exerted by the magnetic-field and by the accretion. The magnetic torque depends on the size and radii of the magnetically connected region to the disk. The radial dependence of  $\gamma_c$  corresponds to the magnetic coupling to the disk. We assumed that the physical mechanism of magnetic diffusion is determined by turbulent diffusion, with which the torque exerted by magnetic-field lines is given by:

---

<sup>2</sup>The break up speed fraction is defined as  $f = \Omega_*/\Omega_{BreakUp}$ , Here its enforced a maximum spin rate of  $f=1$ .

$$\frac{d\tau_m}{dr} = \frac{f^{8/3}\mu^2}{\beta R_*^4} \left(\frac{r}{R_{co}}\right) \left[1 - \left(\frac{r}{R_{co}}\right)^{3/2}\right] \quad (13)$$

where  $\mu$  is the dipole moment, and the radial component  $r$  is neglected. Also the angular momentum carried by the accretion in the disk leads to:

$$\frac{d\tau_a}{dr} = \frac{1}{2}\dot{M}_a f^{3/2} \left(\frac{GM_*}{R_*}\right)^{1/2} \left(\frac{r}{R_{co}}\right)^{-1/2}. \quad (14)$$

Assuming that  $\dot{M}_a$  is constant for all radii, the differential torque at each annulus inside the disk of radial width  $dr$  is:

$$d\tau_i = d\tau_a - d\tau_m \quad (15)$$

this equation represents the transport of angular momentum inside the disk, solving this equation assuming a mechanism of transport of this angular momentum, will solve the structure of the disk, but here we are not interested in the structure of the disk, therefore we assume the equation (15) is valid everywhere.

## 2.5. Truncation Radius

The disk motion follows a keplerian motion. Due to the differential rotation between the disk and the star and the magnetic coupling, the field lines will be twisted. This twisting of the field lines is different for the two regions divided by the corotation radius,  $R_{co}$ , at which radii the disk rotates at the same angular velocity as the star. At smaller radii the magnetic torque tends to extract angular momentum from the disk to the star and beyond  $R_{co}$  the disk removes angular momentum from the star. As can be seen from equation (13) the magnetic torque increases rapidly as one moves towards the star and much more rapidly than accretion torque (14) does. At some point equation (15) will be zero,  $d\tau_a = d\tau_m$ , at such radii the magnetic torque will extract all the angular momentum of the material in these region enabling material to free fall to the star along the field lines maintaining  $\dot{M}_a$  constant. At the left of this radii, the torque is negative, this implies that the angular momentum transfer should be inward, from slower to faster spinning material. Therefore there exist no material in the region where  $d\tau_i < 0$ .

The radius where  $d\tau_a = d\tau_m$  is called truncation radius  $R_t$  and for that radius the angular momentum is injected from the disk to the star. The location of the truncation radius determines the state of the system defined by Matt & Pudritz [22]

### 2.5.1. Truncation Radius Calculation

Replacing equations (14) and (13) into the condition  $d\tau_a = d\tau_m$  the following condition is derived.

$$\left(\frac{R_t}{R_{co}}\right)^{-7/2} \left[1 - \left(\frac{R_t}{R_{co}}\right)^{3/2}\right] = \frac{\beta}{\psi} f^{-7/3} \quad (16)$$

where

$$\psi = 2\mu^2 \dot{M}_a^{-1} (GM_*)^{-1/2} R_*^{-7/2} \quad (17)$$

is a dimensionless parameter that relates the accretion strength with magnetic strength. the numerical calculation of  $R_t$  solves the equation (16) using a Newton-Raphson method. The Truncation radius is always encouraged to be bigger than  $R_*$ , therefore if the magnetic field is not strong enough to truncate the disk and the numerical calculation gives a  $R_t < R_*$  we reset  $R_t = R_*$ .

### 2.5.2. System States

Determining the state of the system depends of the truncation radius, inner radius and outer radius <sup>3</sup> the next figure shows the possible three states of the system.

the first state occurs when the magnetic field is only connected to the region inside  $R_{co}$  and the rest of the field is opened, then we will only have spin down magnetic torque, in this condition we cannot determine the truncation radius as done in the section before, but for our conditions this is not necessary because we will always be in state 2.

the second state of the system, the truncation radius is between the inner radius and the outer radius, and is always smaller than the corotation radius,  $R_t < R_{co}$ , enabling spin up and spin down magnetic torque allowing the equilibrium of torques and the disk-locked state, which is the classical view of the star-disk system.

The last state is when the truncation radius is behind the corotation radius,  $R_t > R_{co}$ , in this state the disk is truncated after the corotation radius therefore there will be no mass accretion, and there will also be no spin up magnetic torque, only spin down magnetic torque, where there is no possibility of equilibrium.

As can be seen with the conditions we are working with, we will always have the truncation radius inside the inner and the outer radius, therefore our system will always be in the second state.

## 2.6. Total Torque

The truncation radius, allows us to compute the accretion torque due to the infall of matter which falls at a velocity equal to the keplerian velocity at  $R_t$ .

$$T_a = \dot{M}_a \sqrt{GM_* R_t} \quad (18)$$

this is known as accretion torque. The magnetic torque enables transport of a significant amount of angular momentum between the star and disk. The general expression for the magnetic torque is shown as eq (21) in [22]<sup>4</sup> but due to our assumption for  $\beta$  and  $\gamma_c$ , the magnetic torque is equal to

$$T_m = \frac{B_*^2 R_*^6}{3\beta R_{co}^3} [-2(R_{co}/R_t)^{3/2} + (R_{co}/R_t)^3] \quad (19)$$

which contains the spin up and spin down torque felt by the star and as we can see, that the magnetic torque depends only on the location of the Truncation radius and the corotation radius. Now the total torque felt by the star is the sum of the accretion torque and the magnetic torque, given by

$$T_* = T_a + T_m \quad (20)$$

This torque neglects any other torque sources that could affect the spin evolution of the star (like stellar wind torques). The system tries to evolve to an equilibrium spin rate, given by  $T_* = 0$ , but as we have already seen, the spin of the system not only depends on this two torques, it also depends on the contraction and the mass of the star.

Given the conditions chosen in this work, with the magnetic field connected to the entire disk, and no field opening, the Total torque will dominate under the changes due to contraction and mass change (i.e. changes in the moment of inertia), this model represents what is known as "Disk-Locking", which leads to spin rates values consistent with the range of observed data.

<sup>3</sup>the inner and outer radius are determined with the twisting of the magnetic field and  $\gamma_c$  and thus with the regions where the field is open. But for our conditions  $\gamma_c = \inf$  so the inner radius is  $R_{in} = R_8$  and  $R_{out} = \inf$ .

<sup>4</sup>Formula for the magnetic torque which depends on the field topology  $\tau_m = \frac{1}{3\beta} \frac{\mu_*^2}{R_{co}^3} [2(1 + \beta\gamma_c)^{-1} - (1 + \beta\gamma_c)^{-2} - 2(R_{co}/R_t)^{3/2} + (R_{co}/R_t)^3]$

## 2.7. Numerical Simulation

Based on the program "history5.c" developed by Matt S. & Pinzón G. [14] we re-wrote it in a different language, c++ and changed the structure of it. The code uses a fourth order Runge-Kutta, which solves the four coupled stellar evolution equations, eq (2)(4)(9)(17) at each timestep. This timestep runs dynamically in order to reduce computational time and increase precision. The main idea of the program is to find the radius, angular velocity, magnetic interaction, torques (accretion and magnetic torques), mass accretion and all of the stellar parameters already discussed. The program solves the same equations and gives the same results, the difference is that this program is written in c++ and is object oriented structured, this was done first because the new language has more libraries and is more commonly used, second because this structure let us distinguish between the private and public variables, this is very important because our private variables are the variables that carry the main information, the stellar parameters variables, and these variables can only be modified by functions from the object class, these functions are supposed to be the main equations for us, in this case the stellar evolution equations, making impossible for the secondary functions that help the program to run, to modify these private values, making the information more classified and safe.

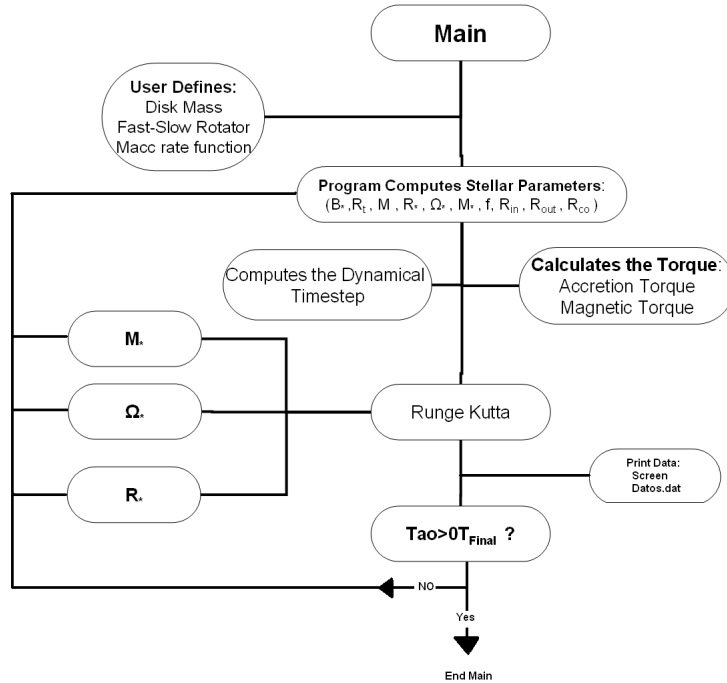
We note that it is useful this new structure of the program, first of all is more appropriate differing class functions from friendly functions and normal functions, it let us to reduce the length of the program, and we won't need to re-write a line of commands to do once again a Newton-Raphson, or a Runge-Kutta. Now we only need to use the appropriate function with the adequate variables to obtain the results we are looking for. It is also easier to understand the program when you see the code as different blocks of structure, first is the class definition, where the class functions and class variables are defined, then the definition of normal functions and the main program is only a few lines which is easier to understand. This code structure makes easier to modify the program for your own purposes by modifying a function, not looking through the whole program changing it but having a big chance to commit a mistake.

The main idea for this change of language and this structure of the program is the possibility to create and add libraries which will function as subprograms to solve a specific case. The main objectives here were to join a program developed by Ramirez Oscar [?], whose program solves the equation for the disk at each point in the space and timestep using a finite differences method, but leaving the rest of the stellar parameters alone, like radius, angular momentum, magnetic field, star-disk interaction, truncation radius, etc. and as we know the "history5.c" solves the stellar evolution equations but using an arbitrary function for the mass accretion. Matching these programs, would let for the first time to have a tool to solve at each timestep the stellar evolution equations and the equations for the disk structure having a nice approximation (third order approximation) for the theoretical mass accretion for a T Tauri star during the first 3 Myr.

Finally I would like to say that this was the first test to reproduce the results obtained by Matt et. al [14], showed in the appendix because of the field topology, in the new language and structure, and it reproduced exactly the same results, it is also working for the open field topology case, but we will not deal with this case in this work and it can be introduced effects like stellar winds to develop a well based code.

## 3. Results

The results of the simulations will be presented by groups, in panels figure [14], first defined by mass accretion model, and then divided by the magnetic field strength. We show 4 graphics in each figure, which are in this order, Break Up Speed Fraction, Period, Truncation & Corotation Radius and Total Torque. The conventions used are red lines for high accretion rates, and black lines for low accretion rates, dashed lines represent high initial angular speed, and solid lines correspond to low initial angular speed. The main difference from these results with the ones presented in [14], are the approach for the mass accretion rate, Power-Law accretion rate is also included based on the measurements done by Hartmann et al [29], the corresponding fit model includes adjustable  $\eta$  parameter, which let us a more realistic description than the exponential or hyperbolic, we can adjust the parameter to reproduce the correlation done by Hartmann 98 [29], or to adjust it based on our needs.



### 3.1. Exponential Accretion

In figure (1) we present the results concerning exponential accretion, the solid Lines represent the exponential accretion, This behaviour is the most intuitive behaviour because we expect the accretion to decrease with time at some rate, not as fast as the power law and neither at a constant rate more like an exponential rate.

The next figure (3) shows the evolution of the different stellar parameters for the low field strength  $B = 500$ . As we see in figure (3 a) the high accretor and slow rotator is the only one who is accelerating for the first  $\sim 10^5 yr$ , the ones with high speed start decelerating and the slow rotator and low accretor has a nearly constant speed, this can be corroborated by looking the figure (3 d), where the torque for the high speed stars is very negative so this will spin down them for the first  $\sim 10^5 yr$  here the magnetic spin down torque dominates over the accretion and spin up magnetic torque which is almost null because the  $R_t \simeq R_{co}$ , the high accretor and slow rotator we see a positive torque component, which comes from accretion and positive magnetic torque due to the region between the  $R_t$  and  $R_{co}$ , so this will spin up the star, and for the slow rotator and low accretor we see a small negative component for the torque, that's why we don't see a lot of variation for these star.

For the next few  $10^5 yr$ , we see a different behaviour, because as can be seen in panel (3 c), the distance between  $R_t$  &  $R_{co}$  is larger, which represents a large region contributing to the spin up magnetic torque, although the accretion torque has diminished, the sum of the spin up magnetic torque and accretion torque overwhelms the spin down contribution of the magnetic torque, which gives rise to positive torques and spin up the stars.

Then at  $10^6 yr$  the accretion torque is close to zero, panel (3 c) shows that the "spin up" region connected is too small so the spin down magnetic torque dominates and spins down the stars for all four cases. As can be seen in panel (3 b) the initial conditions are forgotten but the final period is determined by the total mass accreted into the star, and comparing the final break up speed fraction the high accretors differ in  $\sim 2,8f$  from the low accretors, leaving periods of about 1 – 5 days, which is still being too small in comparison with observations.

Panel (4) compiles the evolution of the four stellar parameters for the same initial conditions as last case, the only variation from the last figure is the strength of the magnetic field, which now is  $B = 2000G$ . Here we can see that the behaviour changes a lot compared to the weak magnetic field case, because here we see that

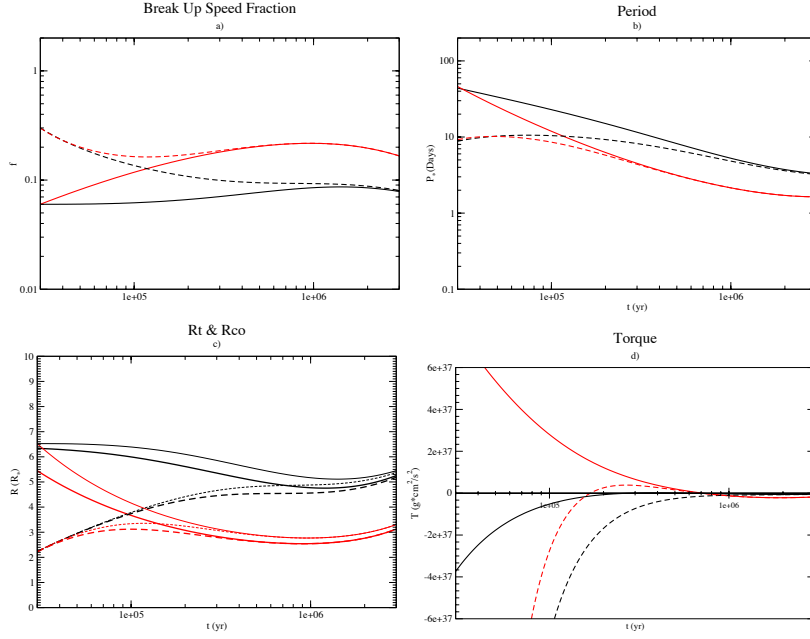


Figure 3: Evolution of the stellar parameters for the Exponential Accretion with  $B = 500G$ , colors correspond red lines for high accretors, black lines for low accretors, solid lines for slow rotators and dashed lines for high rotators. panel a) shows the break up speed fraction for all four cases, b) show the periods c) show the behaviour of the co-rotation radius (thin lines) and truncation radius (thick lines) and d) shows the total torque felt by the star.

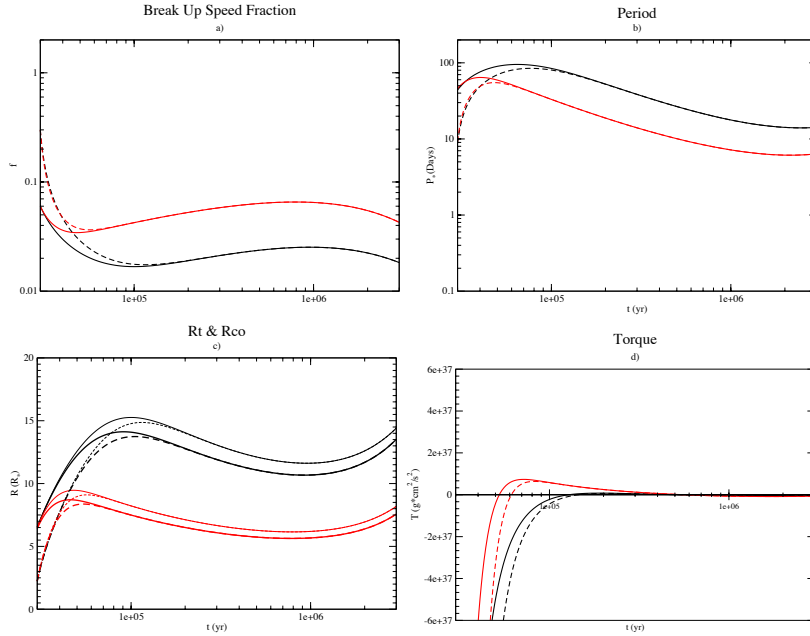


Figure 4: Evolution of the stellar parameters for the Exponential Accretion with  $B = 2000G$ , colors and line types as used in fig (3). panel a) shows the break up speed fraction for all four cases, b) show the periods c) show the behaviour of the co-rotation radius (thin lines) and truncation radius (thick lines) and d) shows the total torque felt by the star.

all the stars, regarding the initial conditions have a drastic deceleration during the first few  $10^5 yr$ , this can be compared with the total torque felt by all the stars, panel (4 d), where we can see that all the stars have big values of negative torque for the first stage, but we can see that this torque is stronger for the fast rotators, than for the slow rotators, even though the accretion torque is strong for the first stages, here the spin down magnetic torque is too strong and for this stage it has no spin up magnetic torque, because as we can see in panel (4 c) there is no region between  $R_t$  and  $R_{co}$  that spins up the star. Then as this region grows, and the accretion torque decrease, the spin up torque turns positive and spin up a little bit the stars, as can be seen in panel (4 a) until  $10^6 yr$ . And finally when the accretion torque is almost null, the spin down magnetic torque dominates again and spins down the star to values around the 10% of the speed-fraction, a difference of about  $\sim 2,5f$  between the low and high accretors is left, which gives periods around 6-20 days, comparable to the observations.

### 3.2. Hyperbolic Accretion

The Hyperbolic accretion is presented with dashed lines in fig 1, this behaviour is nearly constant for the first 2 Myr, and decreases rapidly to an almost null value, this behaviour can seem to be strange because what can cause such an extreme decrease?. This behaviour has been chosen because we wonder about the behaviour of the angular momentum evolution for very different accretion rates and this one is very different to what we Actually This has been seen in some stars, normally massive stars, but it is a known process and we want also to study the effects on TTauri stars. The process that decreases the accretion so fast at  $\sim 2Myr$  is the photoevaporation [29] of the disk, when the radiated photons from the star are sufficiently enough to heat the disk near the star and evaporate them until regions further from co-rotation [30], this decreases the accretion to almost null values.

Panel (5, a) shows the behaviour of the speed for this case. Similar to the Exponential case with  $B = 500$  for all the cases the stars start decelerating, except for the high accretor and low rotator where we see an effective acceleration that can be corroborated with panel (5, d) where torque is positive for almost all simulation, this is due to the constant accretion rate contribution and the spin up magnetic torque which arise from the large region connected to the star between  $R_t$  and  $R_{co}$ . For the rest of the cases in panel (5, c), we can see how this region grows for the next  $\sim 10^5 yr$ , which increases the spin up magnetic torque, and attached to the nearly constant accretion torque, we see that for all the cases we will have a positive torque and thus an acceleration for all four cases.

For the last million year, the accretion decreases rapidly but also the region between  $R_t$  and  $R_{co}$  is minimum which decreases the spin up magnetic torque, thus the total torque will be dominated mostly by the region magnetically connected beneath  $R_{co}$  giving rise to a tail of negative torque, panel(5, d), that spins down the stars for this stage and can be corroborated with panel (5, a), where for all the stars the break up speed fraction has a deceleration tail, where the difference between high and low accretors are around  $\sim 1,8f$ , leaving periods between 1 – 3 Days. This resulting periods are faster than the periods for the case Exponential Accretion and  $B = 500$ , this is due to a longer contribution from a representative accretion torque, because we have the same amount of mass accreted for each case but at a different rate.

For the case of Hyperbolic accretion rate and  $B = 2000$  we can see a similar behaviour to the Exponential Accretion with  $B = 500$  because we see that all the four cases start with a rapid decrease in their speed, fig (6, a), due to a negative torque as shown in fig (6, d), arising from spin down magnetic torque which overwhelms the positive accretion torque, stronger for the fast rotators than for the slow rotators, and spins down the stars near to  $\sim 10\%$  of the break up speed and as can be seen, the initial conditions are forgotten for a few  $\sim 10^5 yr$ .

As the stars are spinning down, the positive magnetic torque starts to increase because the region between  $R_t$  and  $R_{co}$  is also increasing, therefore the positive magnetic torque and positive accretion torque dominates under the negative magnetic torque for all the cases and spins up the stars. The stars keep accelerating with a positive torque until  $\sim 1 \times 10^6 yr$  when the accretion is suddenly stopped decelerating the star and throwing far away the co-rotation radius and also the truncation radius bringing them over progressively vanishing the positive magnetic torque, leaving only negative magnetic torque and therefore a deceleration for the last Myr.

The Resulting periods are constrained between 7 – 20 Days, also seen in the difference in the break up

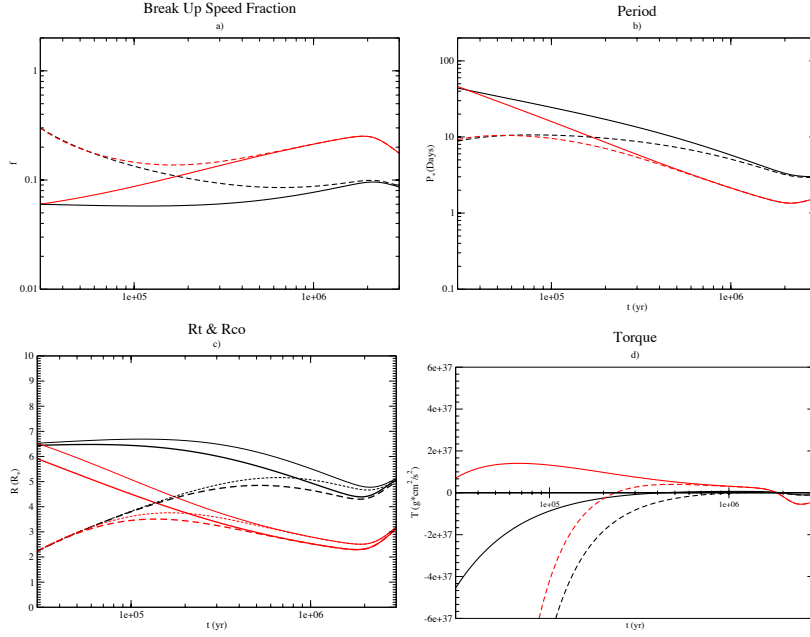


Figure 5: Evolution of the stellar parameters for the Hyperbolic Accretion with  $B = 500G$ . Colors and line types as used in fig (3) panel a) shows the break up speed fraction for all four cases, b) show the periods c) show the behaviour of the co-rotation radius (thin lines) and truncation radius (thick lines) and d) shows the total torque felt by the star.

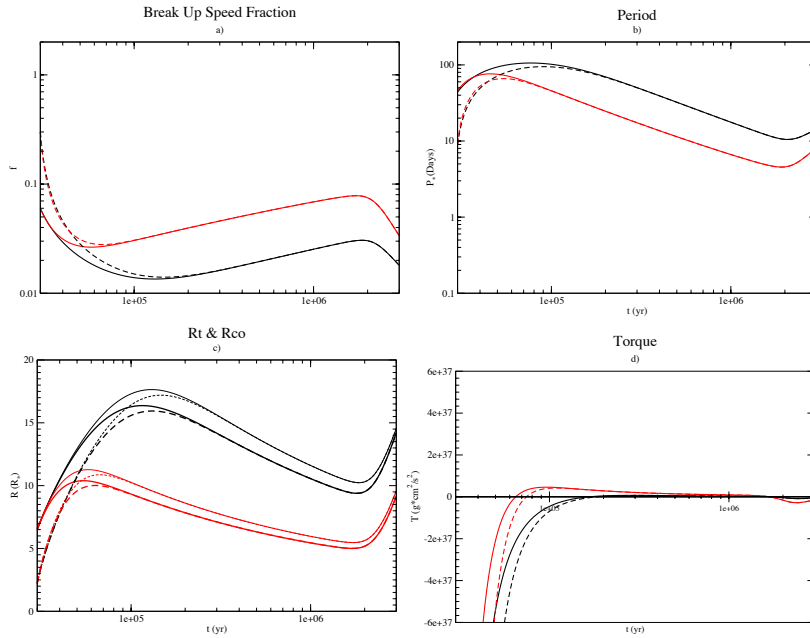


Figure 6: Evolution of the Stellar parameters for Hyperbolic Accretion with  $B = 2000$  using the same conventions in a), b), c) and d) as figure 5



speed fraction which for this case is  $\sim 1,5f$ , this periods are comparable to the observations. A very important comparison between the exponential accretion and hyperbolic accretion with  $B = 2000$  is that for hyperbolic accretion the final velocities for the high accretors and low accretors are closer than for the Exponential accretion, where for exponential accretion the high accretors spins  $0,23f$  faster than the low accretors and for the hyperbolic accretion the high accretors spins  $0,15f$  faster than the low accretors, we can also see that the difference between high accretors and low accretors is smaller for the hyperbolic accretion rate than for the exponential accretion rate of about  $\sim 1f$  for both cases.

### 3.3. Power-Law Accretion

The Power-Law accretion rate was first studied by Hartmann [29], where he adjusted observational data to a power law rate using equation (7), and found that  $1,5 < \eta < 2,8$ , for this case we use  $\eta = 1,8$ <sup>(5)</sup> and its represented in figure (1) as dashed-dotted lines. The Power-Law accretion rate represents a high accretion near the birthline of the star, and almost all disk mass is accreted in the first few  $\sim 10^5 yr$  and the rest of the evolution is primarily dominated by magnetic interaction.

for the first case with  $B = 500$ , figure (7), we see immediately a different behaviour than for the exponential and hyperbolic accretions, for the other two cases we saw that the only condition that showed acceleration was the low rotator and high accretor, but now we see that most of the stars present acceleration for the first years, except for the high rotator and low accretor case. This is clearly seen in panel (7, d), where almost all cases present positive torques for the first few years, but as it is expected the accretion decreases too fast and the magnetic spin down torque dominates the rest of the evolution. Observing the panel (7, d) we corroborate our appreciation of the behaviour for the spin rate, because we see that for most of the cases the separation between  $R_t$  and  $R_{co}$  is too big, giving rise to the spin up magnetic torque, except for the low accretor and high rotator where this difference is negligible, therefore spin down magnetic torque dominates this case. For the next few years we see that the  $R_t$  and  $R_{co}$  get closer to each other and remain closer for the rest of the evolution, such a behaviour is due to the dependence of  $R_t$  by  $\dot{M}$  &  $1/R_{co}$  (16).

As it is clearly seen in panel (7, a) high accretors forget the initial conditions very fast, around  $\sim 1 \times 10^5 yr$ , and maintain a small deceleration for the rest of the evolution reaching equilibrium at almost  $1 Myr$ , leaving a period around 3 days. For the low accretors we see that they forget their initial conditions near 2 Myr, they both decelerate after  $1 \times 10^5 yr$  but at a different rate, which is clearly seen in panel (7, c) and where the torque behaviour is very different for both cases, one starts accelerating and the other one decelerating, until both reach equilibrium at  $\sim 2 \times 10^6 yr$  leaving a period around 5 days. The break up speed difference between the high and low accretors is about  $\sim 2,5f$  almost the same as it is for exponential accretion, but is much more bigger than it is for hyperbolic accretion. The final results for power-law accretion shows that for this rate stars should be spinning slower than for the other cases.

Now for the magnetic field  $B = 2000$  for the power law accretion we don't see too much action because the system reaches the equilibrium very fast, this is because the appreciable accretion disappears in a few thousand years and the magnetic field is very strong so it regulates the system faster towards equilibrium. First we see the panel (8, a) where we see that initial conditions are forgotten in the first  $\sim 3 \times 10^5 yr$ , and then maintain evolving softly until their final spin rates. In panel (8, b) it's clearly seen that they reach almost the final period before  $1 \times 10^6 yr$ , with the bimodal condition of high accretors and low accretors, leaving periods of about 10 – 40 Days which is clearly bigger than the final periods of the exponential and hyperbolic cases and also is bigger the gap between the resulting high and slow rotators. The panel (8, a & b) only corroborate the equilibrium reached by the system, the corotation and truncation radius show that this equilibrium is a magnetic equilibrium, because we know that most of the mass is accreted before  $10^6 yr$ , so accretion torque is not anymore representative in the rest of the evolution, so the system adjusts the truncation radius and corotation radius such that the region connected between those radius, which generates the positive magnetic torque, is big enough to counteract with the spin down magnetic torque due to the connection beyond the corotation radius.

---

<sup>5</sup>Appendix 4.3 has a brief description of the  $\eta$  adjustment done by Hartmann and our own correlation with Hartmann and Pinzón data.

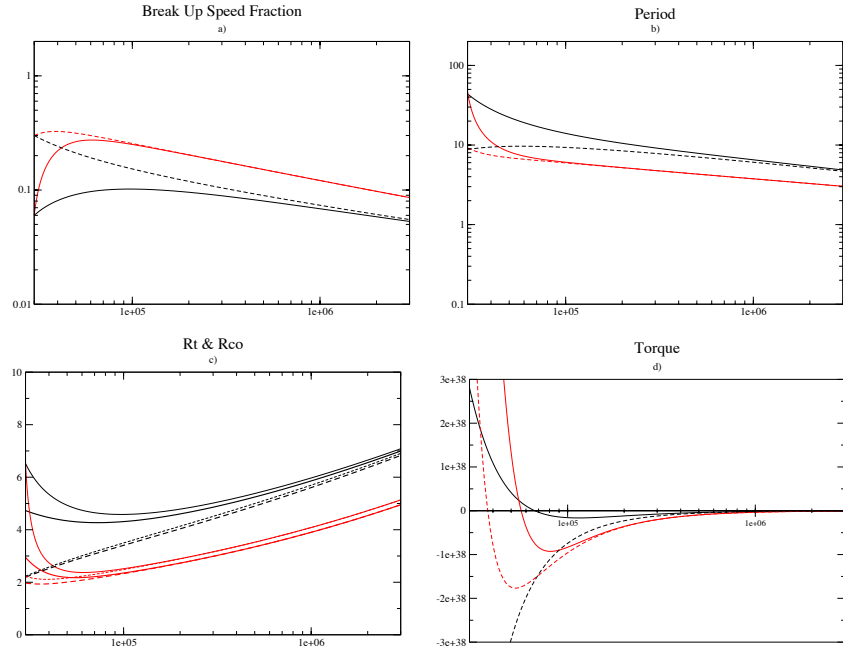


Figure 7: Evolution of the different stellar parameters using the same conventions as 3 now with Power-Law accretion rate and  $B = 500$

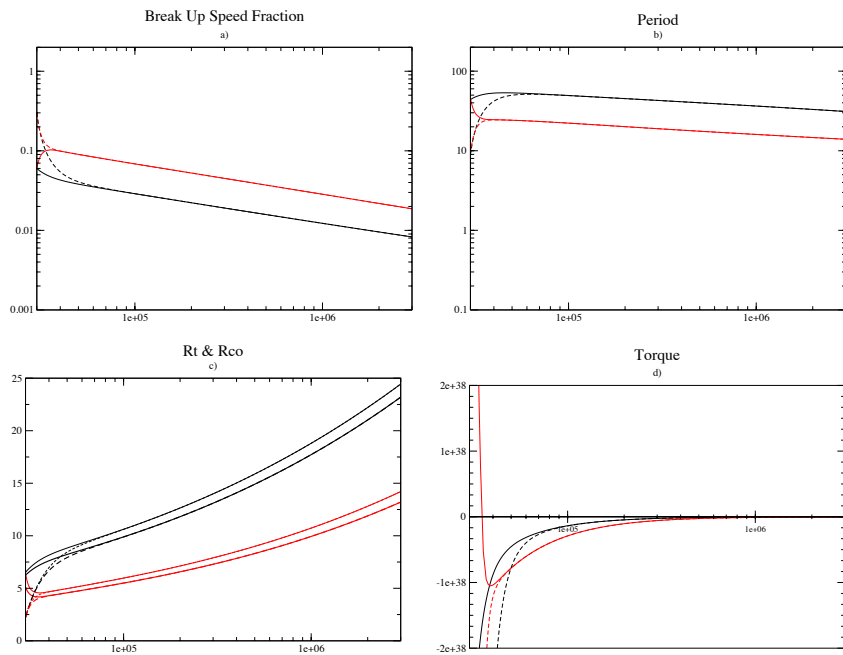


Figure 8: Evolution of the different stellar parameters using the same conventions as 4 now with Power-Law accretion rate and  $B = 2000$

This can be clearly seen in the Torque figure, because first we see that there is a very high accretion where almost all cases have negative torques, except the slow rotator and high accretor which in panel (8, a) is the only one who is accelerating and in panel (8,c) is the only one who has positive magnetic torque contribution, because besides the accretion torque there is only negative magnetic torque, for this cases panel (8,c) shows there is no positive accretion torque. Later on we see that accretion torque is negligible, and magnetic torque dominates the system evolution, and directing the system to an equilibrium.

## 4. Conclusions

We have shown the angular momentum evolution for a T Tauri star during its Hayashi phase evolution, for four different initial conditions, we had fast and slow rotators, and high and low accretors. We used a numerical simulation to iterate the stellar evolution equations for three Myr, using three different functional forms for the mass accretion rate. They were Exponential, Hyperbolic and Power-law accretion rates, these three functions were chosen because each one is very different from the other one, and also it could represent different behaviours. Although we knew we were working with the Classical T Tauri model, we wanted corroborate the necessity of a more complex picture for the angular momentum problem, and it's time to leave behind the " Disk Locking " picture.

As we expected the three functional forms for the mass accretion guided the star to very different behaviours, as can be seen in the torque panels (panel d for all the figures), where we see such a different behaviour of the torque, which is the one who leads the star to equilibrium, this changes from one accretion rate to another, implies how long and strong will torque be exerted on the star, resulting in very different angular velocities. As we expected we have a bimodal behaviour differentiated by magnetic field strength, such bimodality was expected because magnetic torque is the one who spins down the star, so we expect strong magnetic field force stars, to be rotating slower than the weak magnetic field force stars. But another bimodal behaviour was found, this one is ruled by the initial disk mass, low accretors ended rotating at smaller velocities than high accretors. This can be seen in the break up speed fraction panels (The a panels in all the figures.), where the red lines, which are the fast high accretors, are always above the black lines. This implies that the initial angular velocity condition is forgotten, but not the initial disk mass condition. What is very important here is that the hyperbolic accretion rate was the mass accretion function that ended with the closest velocities between high and low accretors and the power-law accretion rate, had the biggest gap between the final velocities of high and low accretors.

Such bimodalities may disappear when a complete and detailed analysis of the processes involved in the star during its Hayashi track evolution is made, because here we have such bimodalities, but we are constrained to lots of hypothesis, which modify the resulting velocities, like the study made by Matt et al [14], where they computed the resulting velocities for four different initial conditions but with the possibility of field opening, and they found once more that the stars were rotating faster than the observational data says. Another critical point is the idea of a functional form for the mass accretion rate, it's much more complicated than that, but solving this problem is the next step to make.

Further visions will come to help us solve this problem, like the presence of stellar winds, different assumptions for the magnetic field, like quadrupolar fields or fields not aligned with the rotational axis, can be included, processes which can be determinants in a complete description of the angular momentum loss in T Tauri stars.

## Referencias

- [1] Joy A. H., ApJ, 1945, 102, 168, 1949, 110, 424
- [2] Walker, M. F. 1972, ApJ, 175, 89
- [3] Lynden-Bell, D. Pringle, J. E. 1974 MNRAS 168, 603
- [4] Bertout, C. 1987, in IAU Symposium, Vol. 122, Circumstellar Matter, ed. I. Appenzeller & C. Jordan, 23-27
- [5] Königl, A. 1991, ApJ, 370, L39
- [6] Ghosh, P. & Lamb, F. K. 1979, ApJ, 232, 259
- [7] Bouvier, J. 1991, in Angular Momentum Evolution of young Stars, ed. S. Catalano & J. R. Stauffer
- [8] Bouvier, J., Bertout, C., Benz, W., Mayor, M., 1986, A&A, 165, 110
- [9] Vogel, S. N. & Kuhl, L. V. 1981, ApJ, 245, 960
- [10] Camenzind, M. 1990, in Reviews in Modern Astronomy, ed. G. Klare, 234-265
- [11] Shu, F., Najita, J., Ostriker, E., Wilkin, F., Ruden, S., & Lizano, S. 1994, ApJ, 429, 781
- [12] Cameron, A. C. & Campbell, C. G. 1993, A&A, 274, 309
- [13] Armitage, P. J. & Clarke, C. J. 1996, MNRAS, 280, 458
- [14] Matt, S. P., Pinzón, G., De La Reza, R., Greene, T. P., Submitted to ApJ,
- [15] Hartmann, L. & MacGregor, K. B. 1982, ApJ, 259, 180
- [16] Mestel, L. 1984, LNP Vol. 193: Cool Stars, Stellar Systems, and the Sun, 193, 49
- [17] Tout, C. A., & Pringle, J. E. 1992, MNRAS, 256, 269
- [18] Matt, S. & Pudritz, R. E. 2005a, ApJ, 632, L135  
Matt, S. & Pudritz, R. E. 2005b, MNRAS, 356, 167  
Matt, S. & Pudritz, R. E. 2008a, ApJ, 678, 1109  
Matt, S. & Pudritz, R. E. 2008b, ApJ, 681, 391
- [19] Edwards, S. 2008, arXiv:0809.3603v1
- [20] Edwards, S. et al. 2003, arXiv:astro-ph/0311289v1
- [21] Insu Yi, 1995, ApJ, 442:768-777
- [22] Matt, S. & Pudritz, R. E. 2005b, MNRAS, 356, 167
- [23] Lynden-Bell, D. & Boily, C. 1994, MNRAS, 267, 146
- [24] Lvelance, R. V. E., Romanova, M. M., & Bisnovatyi-Kogan, G. S. 1995, MNRAS, 275, 244
- [25] Hayashi, M. R., Shibata, K., & Matsumoto, R. 1996, ApJ, 468, L37
- [26] Uzdensky, D. A., Königl, A., & Litwin, C. 2002, ApJ, 565, 1191, van Ballegoijen, A. A. 1994, Space Science Reviews, 68, 299

- [27] Tayler, R.J. 1987, MNRAS, 227, 553
- [28] Rucinski, S. M. 1988, AJ, 95, 1895
- [29] Hartmann, L., Calvet, N., Gullbring, E., & D'Álessio, P. 1998, ApJ, 495, 385
- [30] Matsuyama, Johnstone, and Hollenbach (2009), Dispersal of protoplanetary disks by central wind stripping, ApJ, 700, 10.  
Matsuyama, Johnstone, and Hartmann (2003), Viscous diffusion and photoevaporation of stellar disks, ApJ, 582, 893.
- [31]